

Marc Dandin · Nicole McFarlane ·  
Md Sakibur Sajal ·  
Fahimeh Dehghandehnavi · Babak Nouri

# Single-Photon Avalanche Diodes and Photon Counting Systems

From Phototransduction to Circuit  
Architecture

 Springer

# Single-Photon Avalanche Diodes and Photon Counting Systems

Marc Dandin • Nicole McFarlane •  
Md Sakibur Sajal • Fahimeh Dehghandehnavi •  
Babak Nouri

# Single-Photon Avalanche Diodes and Photon Counting Systems

From Phototransduction to Circuit  
Architecture

 Springer

Marc Dandin  
Carnegie Mellon University  
Pittsburgh, PA, USA

Nicole McFarlane  
University of Tennessee at Knoxville  
Knoxville, TN, USA

Md Sakibur Sajal  
Carnegie Mellon University  
Pittsburgh, PA, USA

Fahimeh Dehghandehnavi  
Carnegie Mellon University  
Pittsburgh, PA, USA

Babak Nouri  
Virginia Tech  
Blacksburg, VA, USA

ISBN 978-3-031-64333-0      ISBN 978-3-031-64334-7 (eBook)  
<https://doi.org/10.1007/978-3-031-64334-7>

© The Editor(s) (if applicable) and The Author(s), under exclusive license to Springer Nature Switzerland AG 2025

This work is subject to copyright. All rights are solely and exclusively licensed by the Publisher, whether the whole or part of the material is concerned, specifically the rights of translation, reprinting, reuse of illustrations, recitation, broadcasting, reproduction on microfilms or in any other physical way, and transmission or information storage and retrieval, electronic adaptation, computer software, or by similar or dissimilar methodology now known or hereafter developed.

The use of general descriptive names, registered names, trademarks, service marks, etc. in this publication does not imply, even in the absence of a specific statement, that such names are exempt from the relevant protective laws and regulations and therefore free for general use.

The publisher, the authors and the editors are safe to assume that the advice and information in this book are believed to be true and accurate at the date of publication. Neither the publisher nor the authors or the editors give a warranty, expressed or implied, with respect to the material contained herein or for any errors or omissions that may have been made. The publisher remains neutral with regard to jurisdictional claims in published maps and institutional affiliations.

This Springer imprint is published by the registered company Springer Nature Switzerland AG  
The registered company address is: Gewerbestrasse 11, 6330 Cham, Switzerland

If disposing of this product, please recycle the paper.

*To Anayiza, Parvin, Hossein, Lyla, Rimi,  
Maliha, Bari, Iza, Noa, Ari, Anya, Sanite,  
Marvel, and Yanick.*

# Preface

There has been significant progress in the development of single-photon avalanche diodes (SPADs) since their inception in the 1970s, yet their use in mainstream applications has lagged behind. In fact, as of the writing of this manuscript, manufacturers of traditional image sensors are only timidly exploring the commercial space for SPADs. Therefore, it is safe to say that despite the advances we have witnessed in the past decades, SPAD technology still has much to prove. Particularly, their integration in complementary metal-oxide semiconductor (CMOS) processes is still an active area of research with many unmet challenges.

Our aim with the present monograph is to contribute to that specific body of knowledge. Therefore, our discussion is restricted solely to CMOS SPADs and to their associated readout and processing circuits. The monograph's scope mirrors that of a tutorial we delivered at the 29th IEEE International Conference on Electronics, Circuits, and Systems (ICECS 2022) held in Glasgow, UK, in December 2022. There, we presented the current state of CMOS SPAD research, and we particularly focused on our own efforts developing perimeter-gated SPADs (pg-SPADs) in standard CMOS technologies. This experience catalyzed this book project, and we are delighted to finally present a monograph that covers SPAD technology from the bottom-up, i.e., starting from fundamental topics like phototransduction and reaching advanced topics like silicon photomultiplier (SiPM) architectures and CMOS imaging with pg-SPADs.

Our target audience includes the curious engineer who has no background in SPAD technology. It also includes SPAD researchers who are eager to explore novel ideas in this field. Each of the book's chapters may be read individually, providing an in-depth view about a particular aspect of CMOS SPAD technology.

Chapter 1 briefly discusses the fundamental notions underpinning photon detection in semiconductor devices. It covers photo-electron emission in semiconductors, noise, and typical photosensor front-end architectures, including Geiger mode front-ends, which include SPAD devices. Chapter 2 covers the issue of premature edge breakdown in SPADs implemented CMOS technologies, and it presents perimeter gating as a viable alternative to mitigate this issue. Chapter 3 focuses on the optoelectronic characterization of CMOS SPADs, covering instrumentation and

measurement strategies. Chapter 4 covers the implementation of a perimeter-gated SPAD imager in a standard CMOS technology. Chapters 5 covers a novel application for SPADs, namely their use in hardware security applications. Chapter 6 discusses silicon photomultipliers, and Chap. 7 reviews readout architectures. Chapter 8 covers dead time correction models. We conclude the book in Chap. 9, summarizing key findings and briefly describing the foreseeable future of pg-SPAD research and development. All throughout, the reader will find a myriad of topics relating to SPADs and photon counting systems in general.

In closing, we hope that the reader will truly enjoy this book and its fresh take on this emerging field. Lastly, we thank our numerous colleagues and students for contributing to this material; they are acknowledged more appropriately in the following *Acknowledgments* section.

Pittsburgh, PA, USA  
Knoxville, TN, USA  
May 2024

Marc Dandin  
Nicole McFarlane

# Acknowledgements

We are indebted to our colleagues and mentors, first, for being a constant source of inspiration, and second, for supporting our interest in optical sensor and microsystems research for nearly two decades. We thank the following individuals for their unwavering support at various points in our journey and to this day. They are: Dr. Larry Pierre, Dr. Pamela Abshire, Dr. Elisabeth Smela, Dr. Robert Fischell, Dr. Honghao Ji, Dr. Akin Akturk, Dr. Valeri Saveliev, Dr. Bathiya Senevirathna, Dr. David Sander, Dr. Kai-Chun Lin, Mr. Sheung Lu, Dr. Khandaker Mamun, Dr. Md. Habib Habib, Dr. Shamim Shawkat, and Mr. Jinlong Gu.

We are also grateful to our students, past and present. We trust that their unfettered enthusiasm and their steadfast engagement will lead to novel avenues in SPAD research, and we are excited to see their growth as the next generation of researchers in this field. We offer special thanks to the students who currently spearhead SPAD efforts in our labs: Mr. Md. Sakibur Sajal, Ms. Fahimeh Dehghandehnavi, Mr. Atik Rahman, Mr. Andalib Nizam, and Ms. Farin Rahman. Generally, we offer our thanks to all the members of our respective research groups, the Integrated Circuits and Bioengineering Laboratory (ICBio Lab) at Carnegie Mellon University, and the M-Lab at the University of Tennessee, Knoxville. We thank them for their intellectual contributions to the many research projects in our portfolios and for their continued trust in our leadership.

We also kindly acknowledge the support of our research administrators without whom none of this work would be possible; our special thanks go to Ms. Jennifer Agnew, Mr. Kevin Bosle, Ms. Allison Ervin, and to Ms. Kristen Geiger and her team, for their support of the ICBio Lab. Lastly, we thank our sponsors for supporting our research and educational endeavors. We particularly acknowledge the United States Department of Energy, the United States National Science Foundation, and Cylab at Carnegie Mellon University for their support.



# Contents

<b>1</b>	<b>Fundamentals of Phototransduction in Semiconductors</b>	1
1.1	Introduction	1
1.2	Photoelectron Emission in Semiconductors	2
1.2.1	Absorption Coefficient	2
1.2.2	Quantum Efficiency	3
1.2.3	Noise	3
1.2.3.1	Shot Noise	4
1.2.3.2	Single-Electron Current in a Vacuum Diode	4
1.2.3.3	Photoelectron Emission Probability in a Time Interval $\tau$	7
1.3	Phototransduction and System-Level Metrics	10
1.4	Photosensor Architectures	11
1.4.1	Photodiode Front Ends	11
1.4.1.1	Photodiode Signal-to-Noise Ratio	11
1.4.2	Avalanche Photodiode Front Ends	14
1.4.2.1	Avalanche Photodiode Signal-to-Noise Ratio	15
1.4.3	Geiger-Mode Avalanche Photodiode Front Ends	16
1.4.3.1	Geiger-Mode APD Noise	18
1.5	Conclusions	18
	References	19
<b>2</b>	<b>Perimeter-Gated Single-Photon Avalanche Diodes</b>	21
2.1	Introduction	21
2.2	Theory of Operation	23
2.2.1	Avalanche Breakdown	23
2.2.2	Low-Light Transduction	24
2.3	Device Architecture	24
2.3.1	Design	24
2.3.2	Rationale	24
2.4	Breakdown Characteristics	25
2.4.1	Experimental Procedures	25
2.4.2	Results	26

- 2.5 Avalanche Photodiode Modeling ..... 29
  - 2.5.1 APD Model ..... 29
- 2.6 Doping Profile Model ..... 30
- 2.7 Simulation and Model Validation ..... 31
- 2.8 Perimeter-Gated SPAD Modeling ..... 33
  - 2.8.1 State-of-the-Art SPAD Modeling Approaches ..... 34
  - 2.8.2 Perimeter-Gated SPAD Theory of Operation ..... 36
  - 2.8.3 Perimeter-Gated SPAD Equivalent Circuit Model ..... 38
- 2.9 Geiger-Mode Readout ..... 41
- 2.10 Conclusions ..... 45
- References ..... 46
- 3 Optoelectronic Characteristics of Perimeter-Gated Single-Photon Avalanche Diodes ..... 51**
  - 3.1 Introduction ..... 51
  - 3.2 Device Architecture ..... 52
    - 3.2.1 Front-End and Readout Circuit Design ..... 52
    - 3.2.2 Readout Circuit Operation ..... 53
  - 3.3 Optoelectronic Characterization ..... 54
    - 3.3.1 Dark Count Rate ..... 54
    - 3.3.2 Signal-to-Noise Ratio ..... 55
    - 3.3.3 Spectral Responsivity ..... 56
      - 3.3.3.1 Experimental Setup and Procedures ..... 57
      - 3.3.3.2 Results ..... 60
    - 3.3.4 Photoresponse Nonuniformity ..... 62
      - 3.3.4.1 Experimental Setup and Procedures ..... 64
      - 3.3.4.2 Single-Pixel Spectral Responsivity Measurement ..... 65
      - 3.3.4.3 Photoresponse Nonuniformity Measurement ..... 67
      - 3.3.4.4 Results ..... 69
  - 3.4 Conclusions ..... 70
  - References ..... 70
- 4 Perimeter-Gated Single-Photon Avalanche Diode Imagers ..... 73**
  - 4.1 Introduction ..... 73
  - 4.2 Imager Architecture and Operation ..... 75
  - 4.3 Theory and Background ..... 78
    - 4.3.1 Image Formation ..... 78
    - 4.3.2 Elimination of DSNU with Perimeter Gating ..... 78
    - 4.3.3 Effects on PRNU from Perimeter Gating ..... 79
    - 4.3.4 Fixed Pattern Noise Compensation ..... 80
      - 4.3.4.1 Two-Point Calibration ..... 81
      - 4.3.4.2 Wavelet Decomposition ..... 82
      - 4.3.4.3 Multichannel Least Mean Square (mLMS) ..... 83
  - 4.4 Results and Discussion ..... 84
    - 4.4.1 Reduction of Nonuniformity with Perimeter Gating ..... 84

4.4.2	Raw Image Acquisition at Varying Gate Voltages .....	85
4.4.3	FPN Correction .....	85
4.4.3.1	Calibration and Filtered-Based Methods .....	86
4.4.3.2	McLMS Correction .....	86
4.5	Conclusions .....	87
	References .....	88
<b>5</b>	<b>Perimeter-Gated Single-Photon Avalanche Diode Arrays as Hardware Security Primitives .....</b>	<b>91</b>
5.1	Introduction .....	91
5.2	Imager Operation and Key Generation .....	93
5.2.1	Imager Operation in the PUF Mode .....	93
5.2.2	Fingerprint and Key Generation .....	94
5.3	Experimental Validation and Discussion .....	96
5.4	Challenge Response Pair Enhancement .....	98
5.4.1	Limitations of State-of-the-Art Imager PUFs .....	99
5.4.2	Proposed Technique .....	101
5.5	Measured Results .....	101
5.5.1	CRP Without Perimeter Gate Control .....	101
5.5.2	CRP Enhancement with PUF Reconfiguration .....	102
5.5.3	Key Generation and Quality Assessment .....	103
5.5.4	Temperature Resiliency .....	104
5.6	True Random Number Generation Using pg-SPADs .....	104
5.7	Related Works .....	105
5.8	Device Operation .....	106
5.9	Implementation and Measured Results .....	107
5.9.1	Perimeter Gating Achieves Equiprobable Binary States ....	107
5.9.2	Experimental Methods .....	108
5.9.3	Bit Distribution and RBE Around the Optimal Gate Voltage .....	109
5.9.4	NIST Randomness Tests .....	110
5.9.5	Perimeter Gating Compensates for Temperature Change ...	112
5.10	Conclusions .....	112
	References .....	112
<b>6</b>	<b>Silicon Photomultipliers .....</b>	<b>117</b>
6.1	Introduction .....	117
6.2	18 × 18 Analog SiPM Array .....	118
6.3	pg-SPAD SiPM Characterization .....	119
6.3.1	pg-SPAD Breakdown Voltage .....	119
6.3.2	pg-SPAD SiPM I-V Characterization .....	120
6.3.3	pg-SPAD SiPM: Optical Characterization .....	120
6.3.4	pg-SPAD SiPM: Temperature Characterization .....	124
6.4	Dead Time Reduction Strategies .....	126
6.4.1	Circuit Techniques for Dead Time Reduction .....	127
6.4.2	Reduced Dead Time Pixel .....	128

6.5	Conclusions .....	132
	References .....	132
<b>7</b>	<b>Readout Strategies and Asynchronous Architectures</b> .....	<b>135</b>
7.1	Introduction .....	135
7.2	Preamplifier Structure in Nuclear Imaging Systems .....	138
	7.2.1 Charge-Sensitive Preamplifiers (CSPs).....	139
	7.2.2 Transimpedance Preamplifier .....	140
	7.2.3 Voltage-Sensitive Preamplifiers.....	142
7.3	Energy Measurements .....	143
7.4	Timing Measurements .....	146
7.5	Position Sensing .....	148
7.6	Array Readout .....	149
7.7	Conclusions .....	150
	References .....	151
<b>8</b>	<b>Dead Time Correction in Single-Photon Avalanche Diode</b>	
	<b>Front Ends</b> .....	<b>165</b>
8.1	Introduction .....	165
8.2	Theoretical Framework .....	166
	8.2.1 Standard Count Rate Correction Model .....	166
	8.2.2 Proposed Count Rate Correction Model .....	168
8.3	Experimental Methods .....	170
	8.3.1 Perimeter-Gated Single-Photon Avalanche Diode and Equivalent Circuit Model.....	170
	8.3.2 Front-End Interface and Readout Circuit for Studying Dead Time .....	173
	8.3.3 Active Quenching and Active Reset Functionalities.....	173
	8.3.4 Adjustable Output Pulse Width Generation Circuit .....	175
8.4	Measured Results .....	176
8.5	Conclusions .....	177
	References .....	177
<b>9</b>	<b>Conclusions, Contributions, and Future Work</b> .....	<b>179</b>
9.1	Conclusions and Contributions .....	180
9.2	Future Work.....	181
	<b>Index</b> .....	<b>183</b>

# Acronyms

ADC	Analog-to-digital converter
AER	Address event representation
APD	Avalanche photodiode
APS	Active pixel sensor
AQAR	Active quench active reset
BiCMOS	Bipolar complementary metal-oxide semiconductor
BJT	Bipolar junction transistor
CCD	Charge-coupled device
CFD	Constant fraction discriminator
CFPN	Column fixed-pattern noise
CMFB	Common mode feedback
CMOS	Complementary metal-oxide semiconductor
CRP	Challenge-response pair
CSP	Charge-sensitive pre-amplifier
CTR	Coincidence time resolution
DAQ	Data acquisition
DC	Direct current
DCM	Dark count map
DCR	Dark count rate
DCT	Discrete cosine transform
DNF	Denoised figure
DSNU	Dark signal non-uniformity
DUT	Device under test
EMVA	European Machine Vision Association
EVG	Event generator
FLIM	Fluorescence lifetime imaging microscopy
FPGA	Field-programmable gate array
FPN	Fixed-pattern noise
FWHM	Full-width half-max
GMAPD	Geiger mode avalanche photodiode
HD	Hamming distance

ICECS	(IEEE) International Conference on Electronics, Circuits, and Systems
IOT	Internet-of-things
JFET	Junction field-effect transistor
KDC	Key distribution center
LED	Leading edge discriminator
LIDAR	Light detection and ranging
LOC	Lab-on-a-chip
LYSO	Lutetium–yttrium oxyorthosilicate
MCLMS	Multichannel least mean square
MEMS	Micro-electro-mechanical systems
MOSFET	Metal-oxide field-effect transistor
MSE	Mean square error
NEP	Noise-equivalent power
NHD	Normalized Hamming Distance
NIST	National Institute of Standards and Technology
PCB	Printed circuit board
PD	Photo detector
PDE	Photo detection efficiency
PEB	Premature edge breakdown
PET	Positron emission tomography
PG-SPAD	Perimeter-gated single-photon avalanche diodes
PMT	Photo-multiplier tube
PRNG	Pseudo-random number generator
PRNU	Photoresponse non-uniformity
PUF	Physically unclonable function
PZC	Pole zero cancellation
QLC	Quenching logic circuit
RBE	Random bit efficiency
RLC	Reset logic circuit
RNG	Random number generator
ROC	Readout circuit
SAR	Successive approximation register (ADC)
SCD	Symmetric charge division multiplexing
SIPM	Silicon photomultiplier
SNR	Signal-to-noise ratio
SPAD	Single-photon avalanche diode
STI	Shallow trench isolation
STS	Statistical test suite
SMU	Source measure unit
TAC	Time-to-amplitude converter
TDC	Time-to-digital converter
TIA	Transimpedance amplifier
TOT	Time-over-threshold
TRNG	True random number generator
VDE	Variable delay element

# Chapter 1

## Fundamentals of Phototransduction in Semiconductors



### 1.1 Introduction

The study of the interaction of light with semiconductors is extensive; in this chapter we provide only the fundamental notions that are necessary to understand the operation of a photosensor.<sup>1</sup> Our discussion begins with the physical mechanism underlying the conversion of photons to free carriers in a semiconductor material. This process, which is referred to as photogeneration or photoelectric emission, is at the core of imaging science, and a thorough understanding of its nature is required when designing the front end and the readout chain [1].

We then center our discussion on the concept of phototransduction and on a set of system-level performance metrics, namely, the SNR, the noise equivalent power (NEP), and the spectral responsivity ( $S(\lambda)$ ). Taken together, these figures of merit provide important insights into device performance by allowing the identification, at the design stage, of the trade-offs that exist between various circuit parameters. To illustrate this fact and also to understand the operation of the SPADs and pg-SPADs featured in this book, we focus on three distinct photosensor configurations, namely, the photodiode, the avalanche photodiode, and the single-photon avalanche photodiode configuration.

---

<sup>1</sup> Here, the term photosensor is used to designate the front-end (i.e., the detector) and the readout circuit (ROC).

## 1.2 Photoelectron Emission in Semiconductors

### 1.2.1 Absorption Coefficient

The transmission of light through a semiconductor is governed by the Beer-Lambert law (shown below) [2]. It states that within the material, an incident light beam (of intensity  $I_{IN}$ ) is attenuated by an exponential factor that depends on the material's thickness ( $d$ ) and on a wavelength-dependent parameter  $\alpha$ , the absorption coefficient. Thus, the exiting light beam (of intensity  $I_{OUT}$ ) has a smaller intensity than the incident beam. Figure 1.1 shows the absorption coefficient data for commonly used semiconductors.

$$I_{OUT} = I_{IN}e^{-\alpha d}. \quad (1.1)$$

If the incident photons have enough energy, they will cause the valence electrons to migrate to the conduction band. These band-to-band transitions occur only when the incoming photons have energies that exceed the band gap energy of the semiconductor [2]; otherwise, the photons pass through the material.

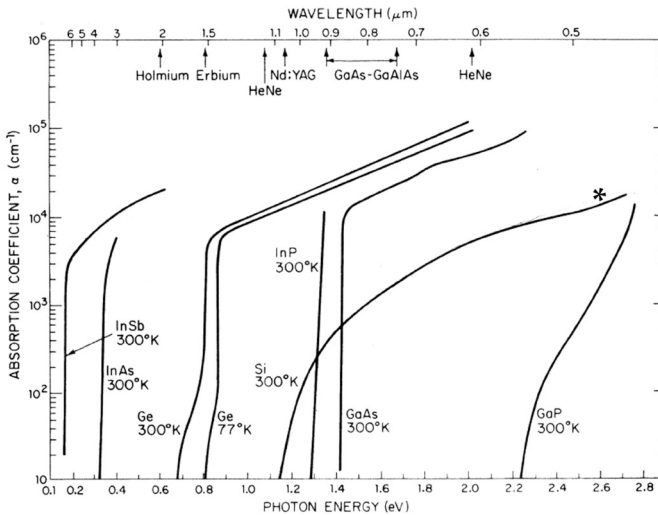


**Fig. 1.1** Absorption coefficient of different semiconductor materials as a function of photon energy and wavelength. The asterisk indicates the data for silicon, the material with which the detectors featured in this book were fabricated. (Figure adapted from ref. [2])



### 1.2.2 *Quantum Efficiency*

Once photons are absorbed, they generate charge with an efficiency factor denoted  $\eta$ . This *quantum* efficiency is an important metric in detector design. It is the ratio of the number of photoelectrons generated to the number of photons incident on the material. Since photon absorption is wavelength-dependent as shown above, so is  $\eta$ .<sup>2</sup> Moreover, it also depends on the reflection coefficient ( $R$ ) of the interface formed by the medium in which the incident light originates and the semiconductor's surface [4].

### 1.2.3 *Noise*

Here we cursorily introduce the concept of noise. We refer to noise as the sum of the effects of secondary physical processes that contribute to the detector's signal, the primary process here being the absorption and transduction of the photons of interest. Such secondary processes may include the thermal generation of carriers, band-to-band tunneling, or releases from trapped carriers. There are also sources of noise in the readout chain, and these do also contribute to the overall noise associated with the phototransduction process. Furthermore, the uncertainty in the impinging light itself may give rise to a noisy signal; this process is termed *shot noise*, and it is described in detail below.

For ease of analysis, we focus only on the detector front end for now, i.e., we do not consider readout noise processes. Let us first consider how carriers are generated in the detector during phototransduction; this happens via photoelectric emission in which electrons jump from the valence to the conduction band.

An ensemble measurement of the number of photogenerated carriers will show a spread around a mean value. This uncertainty is the aggregate result of several noise phenomena originating from one or more of the processes mentioned above. In a traditional detector, the two most important source of noise can be the inherent randomness in the impinging light quanta, i.e., the shot noise, and the random motion of charges due to thermal energy [4].

While the latter effect can be mitigated by cooling the detector and actively regulating the ambient temperature, the former cannot be suppressed. Shot noise is the fundamental noise limit of photodetection, and it sets a lower bound to the noise figure of optical sensing circuits [3, 4]. Because of its importance, we spend some

---

<sup>2</sup> If the incoming light is modulated, the quantum efficiency also depends on the modulation frequency. This dependence is not fundamental; rather it is related to circuit and device parameters (see [3]). Thus, for completeness, the quantum efficiency is denoted  $\eta(\lambda, w)$ , where  $\lambda$  is the photon's wavelength and  $w$  the modulation frequency.

time in the following section analyzing its origin, and we formulate a relationship for it, which we will use in our front-end models in the remainder of this chapter. The analysis featured is credited to Davenport and Root [5], and although a vacuum diode was used as a model for arriving at the result, the analysis extends well to all photosensor front ends.

### 1.2.3.1 Shot Noise

In an optical sensor front end, the photogenerated current exhibits random fluctuations that are independent of the ROC noise sources and of thermal energy. These fluctuations are known as the shot noise, and they arise from the discrete and random removal of energy quanta from the incident radiation field. For this reason, shot noise is a quantum mechanical random process, and it is the fundamental noise which underlies all light detection and measurement applications.

In a detector that integrates photogenerated charge, like an active pixel sensor (APS), for example, the shot noise manifests itself as an uncertainty in the source follower-buffered voltage of the integration node. On the other hand, in a detector that performs photoelectric counting, like the pg-SPAD, it can be estimated from the uncertainty in the count rate.

Thus, the number of photoelectrons generated in a detector is a random process, irrespective of the detector's mode of operation and architecture. The distribution that describes this random process can be derived by considering photoelectron emission in an ideal vacuum photocathode (shown in Fig. 1.2).

### 1.2.3.2 Single-Electron Current in a Vacuum Diode

In Fig. 1.2a the plate (or anode) is biased at a constant voltage denoted  $V_A$  and the photocathode is held at ground. This system is governed by the following electrostatic and classical kinematic equations:

$$\mathbf{F}_m = m\mathbf{a} \quad (1.2)$$

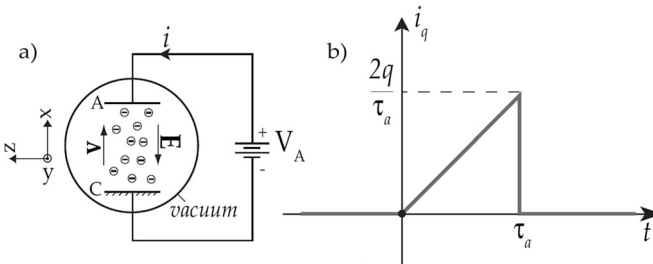


**Fig. 1.2** (a) Vacuum photodiode. (b) Single-electron current pulse

$$\mathbf{F}_l = -q\mathbf{E} \quad (1.3)$$

$$\mathbf{E} = -\nabla V \quad (1.4)$$

$$\nabla^2 V = -\frac{\rho}{\epsilon} \quad (1.5)$$

$$\mathbf{J} = \rho \mathbf{v} \quad (1.6)$$

Here,  $\mathbf{F}_m$  is the Newtonian force that a moving electron is subjected to as a result of its acceleration through the electric field  $\mathbf{E}$  resulting from the potential difference between the two electrodes,  $\rho$  is the charge density,  $\mathbf{J}$  the current density, and  $\mathbf{v}$  the velocity of the electron.  $\mathbf{F}_l$  is the Lorentz force in the absence of a magnetic field ( $\mathbf{B} = 0$ ).

We first solve for the potential as a function of distance. We restrict our analysis to only one dimension, that is, the y and z components of the E-field are zero. We further assume that temperature is constant and that there are no space charge effects. The latter assumption means that the electron does not interact with other electrons during its motion and that its initial velocity, in comparison to its terminal velocity (at the plate), is negligible. Consequently, Poisson's equation (1.5) simplifies to Laplace's equation ( $\nabla^2 V = 0$ ). This yields the boundary value problem (Eqs. 1.7, 1.8, and 1.9) whose solution is shown in Eq. 1.10:

$$\frac{\delta^2 V}{\delta x^2} = 0 \quad (1.7)$$

$$V(0) = 0 \quad (1.8)$$

$$V(d) = V_A \quad (1.9)$$

$$V(x) = \frac{V_A}{d}x \quad (1.10)$$

The electric field is obtained using Eq. 1.4. In Eq. 1.11, the vector  $\hat{\mathbf{i}}$  indicates the basis vector in the x-direction in a Cartesian reference frame:

$$\mathbf{E} = -\frac{V_A}{d}\hat{\mathbf{i}} \quad (1.11)$$

We may now find a second-order differential that describes the motion of the electron by using a force balance equation. This is done by equating the Lorentz force to the Newtonian force. This yields

$$\mathbf{F}_l = \mathbf{F}_m \quad (1.12)$$